

Constraints on variations in inflaton decay rate from modulated preheating

Arindam Mazumdar,^a Kamakshya Prasad Modak^b

^aTheory Division, Saha Institute of Nuclear Physics, Kolkata-64, India

^bAstroparticle Physics and Cosmology Division, Saha Institute of Nuclear Physics, Kolkata-64, India

E-mail: arindam.mazumdar@saha.ac.in, kamakshya.modak@saha.ac.in

Abstract. Modulated (p)reheating is thought to be an alternative mechanism for producing super-horizon curvature perturbations in CMB. But large non-gaussianity and iso-curvature perturbations produced by this mechanism rule out its acceptability as the sole process responsible for generating CMB perturbations. We explore the situation where CMB perturbations are mostly generated by usual quantum fluctuations of inflaton during inflation, but a modulated coupling constant between inflaton and a secondary scalar affects the preheating process and produces some extra curvature perturbations. If the modulating scalar field is considered to be a dark matter candidate, coupling constant between the fields has to be unnaturally fine tuned in order to keep the local-form non-gaussianity and the amplitude of iso-curvature perturbations within observational limit; otherwise parameters of the models have to be tightly constrained. Those constraints imply that the curvature perturbations generated by modulated preheating should be less than 15% of the total observed CMB perturbations. On the other hand if the modulating scalar field is not a dark matter candidate, parameters of the models could not be constrained, but the constraints on the maximum amount of the curvature perturbations coming from modulated preheating remain valid.

Contents

1	Introduction	1
2	Dynamics of fields	2
3	Amplitude of curvature perturbation	4
3.1	Derivation	4
3.2	Constraints	9
4	Iso-curvature perturbation	10
5	Non-gaussianity	11
6	Conclusion	15
A	Numerical details	16

1 Introduction

Production of curvature perturbation during early stage of the universe is mainly described as a mechanism of quantum fluctuation generated at the time of inflation [1, 2]. But there is an equally possible theory of generating density perturbations via variations in the decay rate of inflaton field after the end of inflation [3–7]. There are some models in particle physics and string theories [8–10] where a non-renormalizable interaction term in the Lagrangian ensures that the decay rate for that channel varies depending on the vacuum expectation value (vev) of a spectator field in a particular Hubble patch. So in different disconnected Hubble patches the inflaton decays at different rates which produces curvature perturbations on super horizon scales. In this paper we study both semi-analytically and numerically how changes in coupling of the inflaton field with another secondary scalar field affects the number of e -foldings during preheating process. Using the δN approximation or “separate universe” approach [11–13] we determine the curvature perturbations produced in this period. We constrain the parameters of the Lagrangian from different observables of cosmic microwave background (CMB).

There are three different observables that can put constraints on the model parameters. First is the amplitude of curvature perturbations created by this mechanism. Second one is the amplitude of iso-curvature perturbations generated during modulated preheating. And third one is the non-gaussianity produced in this era.

Variations in the decay rate of inflaton have been mainly studied in the context of modulated reheating scenario [3, 4, 14–17]. The term “modulated preheating” was first coined by the authors of Ref. [18]. But in their calculations preheating was studied without taking into account the effect of backreaction. Later the authors of Ref. [19] have studied it extensively considering the backreaction effect. They have found that the amplitude of curvature perturbations varies non-trivially with the change in the coupling constant (g) between the inflaton field (ϕ) and the secondary scalar field (χ). The reason behind this has been pointed out to be the non-trivial dependence of Floquet exponent (μ_k) with g . Here we study the variation of curvature perturbations with coupling constant g using lattice simulation and develop an analytical tool which correctly reproduces the order of magnitude of curvature perturbations coming from lattice simulation. We find that the non-trivial dependence of curvature perturbations is there in the results of lattice simulation too. But the variation in g need to be tightly constrained in order that the amplitude

of curvature perturbations remain within the observational limit. To constrain different parameters we have been guided by the philosophy that while building any model of physics, the value of any particular parameter should not be fine tuned to produce the observational results. Therefore if we assume some particular dependence of g on the vev of a modulating scalar and a cutoff scale, both of them can be constrained from the value of iso-curvature perturbations and non-gaussianity.

The paper is organized as follows. In section 2 we discuss the general mechanism of modulated preheating and dynamics of different fields. In section 3 we develop the tool for semi-analytical estimation of the curvature perturbations via δN formulation in subsection 3.1. We also provide the lattice simulation results of δN and its derivatives in this subsection. In subsection 3.2 we show the constraints on the variations in coupling constant coming from the amplitude of curvature perturbations. The calculation of possible iso-curvature perturbations produced in this era has been shown in section 4 and necessary constraints have also been set. Amount of local form non-gaussianity yielded by this mechanism has been estimated in section 5 and constraints on model parameters have been derived following the latest Planck results. We finally sum up our findings and conclude in section 6. Necessary numerical details are provided in an appendix A. Throughout the paper we will use the units in which Planck mass $M_P = 1/\sqrt{G} = 1$.

2 Dynamics of fields

We take the simple $m^2\phi^2$ inflaton potential for studying preheating mechanism. If there is no modulation on the coupling constant between inflaton ϕ and a secondary field χ the potential can be written as

$$V(\phi) = \frac{1}{2}m^2\phi^2 + \frac{1}{2}g^2\phi^2\chi^2. \quad (2.1)$$

After inflation ϕ oscillates around the minima of the potential. This oscillation pumps up the production of χ particle. The amplitude of classical background of ϕ decreases as $\phi = \phi_0 a^{-3/2}(t)$ where a is the scale factor. Thus $\Phi(t) = \phi(t)a^{3/2}(t)$ maintains constant amplitude and has a form like,

$$\Phi(t) = \phi_0 \cos(mt). \quad (2.2)$$

We assume that the χ field does not have any classical background value. Rescaling the χ field as $X = a^{3/2}(t)\chi$, we find that the Klein-Gordon equation of X turns out to be in form of the Mathieu equation,

$$\ddot{X}_k + (A_k + 2q \cos(2t)) X_k = 0, \quad (2.3)$$

where derivative has been taken in terms of mt , and

$$\begin{aligned} A_k &= \frac{k^2}{a^2 m^2} + 2q, \\ q &= \frac{g^2 \phi_0^2}{4m^2}. \end{aligned} \quad (2.4)$$

Solution of X_k has the form of $e^{\mu_k mt}$ where μ_k is the Floquet exponent and it is a function of A_k and q .

But if there is another scalar spectator field σ and it is coupled to χ through some interaction term in the Lagrangian, the effective coupling between ϕ and χ varies depending on the value of the vev of σ in a particular Hubble patch. Let us take an example of a particular type of dependence of g on σ . In Ref. [20] the following potential was assumed

$$V(\phi, \sigma, \chi) = \frac{1}{2}m^2\phi^2 + \frac{1}{2}g_0^2\phi^2\chi^2 + \xi\chi^2\sigma + \frac{\lambda}{2}\chi^2\sigma^2 + \frac{1}{2}m_\sigma^2\sigma^2, \quad (2.5)$$

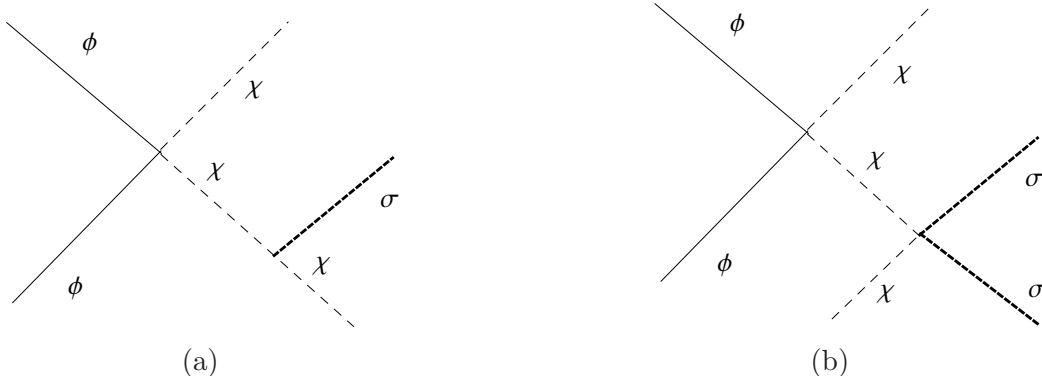


Figure 1. (a) If there is no Z_2 symmetry imposed on σ , this kind of interaction will give rise to the dim-5 operator of Eq. (2.6). (b) For the opposite case the dim-6 operator of Eq. (2.7) can be generated through this interaction.

where ξ and λ are coupling constants. If no particular symmetry is imposed on this potential for the field σ , the second term and the third term of RHS of Eq. (2.5) can generate the interaction shown in Fig. 1-(a). This interaction can be thought of as a process to be produced by an effective interaction term in the Lagrangian involving two ϕ fields, two χ fields and one σ field. This effective interaction is inversely proportional to the square of the mass (M_χ) of the intermediate scalar field (χ) in the low energy limit. Therefore, the lowest order non-renormalizable interaction involving ϕ , χ and σ can be written as

$$g_0^2 \xi \frac{1}{M_\chi^2} \sigma \phi^2 \chi^2. \quad (2.6)$$

The mass of χ field comes from the vevs of ϕ and σ .

Now, if we impose a Z_2 symmetry on σ , the term $\xi \chi^2 \sigma$ will no longer remain in Eq. (2.5). Therefore, the higher order interaction will be generated from $\frac{1}{2} g_0^2 \phi^2 \chi^2$ and $\frac{\lambda}{2} \chi^2 \sigma^2$ terms as shown by the diagram Fig. 1-(b). Hence the lowest order non-renormalizable interaction would become

$$\frac{g_0^2 \lambda}{M_\chi^2} \sigma^2 \phi^2 \chi^2. \quad (2.7)$$

But this is not the only type of mechanism which can generate σ dependent coupling constant. In more realistic models fermion loops can also generate such non-renormalizable interactions. In string theories compactification of higher dimensions can generate modulated coupling constant[8]. Therefore without going into the details of any particular model we keep it general and take effective coupling g for Eq. (2.6) types of cases as

$$g^2 = g_0^2 \left(1 + \frac{\langle \sigma \rangle}{M_1} \right), \quad (2.8)$$

and for the case of Eq. (2.7) it would look like

$$g^2 = g_0^2 \left(1 + \frac{\langle \sigma \rangle^2}{M_2^2} \right). \quad (2.9)$$

Here M_1 and M_2 are two different mass scales and $\langle \sigma \rangle$ is the classical background value of the field σ .

We take m_σ to be much much smaller than m to keep σ field light during inflation. This will allow inflation to generate super-horizon perturbations of σ . If $\langle \sigma \rangle$ is of the order of ϕ its potential energy will

be negligible compared to $\frac{1}{2}m^2\phi^2$ and $\langle\sigma\rangle$ would be frozen. Therefore we can expect the value of $\langle\sigma\rangle$ to be of same order in the era of inflation and preheating.

The values of M_1 and M_2 determines whether the σ field would gain sufficiently large amplitude, comparable to that of χ , at the time of preheating. Let us make an order of magnitude estimate. It has been shown that [21] to have efficient preheating g^2 should be of the order of $10^5 m^2$. The effective couplings between ϕ and σ are $g_0^2 \frac{\langle\chi^2\rangle}{M_1}$ and $g_0^2 \frac{\langle\chi^2\rangle}{M_2}$ for two above mentioned cases. Typical value of $\langle\chi^2\rangle$ in any Hubble patch is of the order of 10^{-14} at the time of the start of preheating[21]¹. If we take g_0^2 to be of the order of $10^5 m^2$ we need to have $M_2 \approx 10^{-7}$ and $M_1 \approx 10^{-14}$ to make both the fields χ and σ experience parametric resonance. But when M_2 and M_1 have much higher values than these, only χ would undergo parametric resonance and σ won't. After a few oscillations of ϕ , $\langle\chi^2\rangle$ might be large enough to start parametric resonance in σ , but since the growth of fields under parametric resonance is exponential it would be too late for $\delta\sigma$ to catch up with the order of χ .

The Second concern is that whether decay of χ into σ would influence the parametric resonance of χ . In Ref.[22] it had been numerically shown that it does not. Therefore if we do not take small values of M_1 and M_2 , σ can only show its effect on the parametric resonance of χ if it has a large finite vev $\langle\sigma\rangle$. In this way it would modify the effective coupling constants of Eq. (2.8) and Eq. (2.9). Since m_σ is negligible compared to H throughout inflation and preheating, motion of the classical background of σ would be over damped. Therefore we can assume that the vev $\langle\sigma\rangle$ is not very different in inflation era and preheating era.

So, for studying the modulated preheating in different Hubble patches of the universe we can only solve the parametric resonance of Eq. (2.3) with different values of g . $\langle\sigma\rangle$ is the combination of the background value of σ at the time of horizon-exit of the largest mode of CMB, say $\langle\sigma\rangle^*$ and its super-horizon perturbations $\delta\sigma$.

$$\langle\sigma\rangle = \langle\sigma\rangle^* + \delta\sigma . \quad (2.10)$$

Therefore $\delta\sigma$ ensures the change in $\langle\sigma\rangle$ in different Hubble patches and the variation in $\langle\sigma\rangle$ is responsible for the variation in g . So Floquet exponent μ_k also varies in different regions of the universe giving rise to difference in the time required to finish preheating. This difference in final time of preheating generates difference in the number of e -foldings N in different ‘‘seperate universes’’.

3 Amplitude of curvature perturbation

In this section we will derive the amplitude of curvature perturbations both semi-analytically and numerically. Then we will compare these two results and we will also compare our semi-analytical result with that of an earlier work. In a subsection, the constraint coming out of the observation on the variation of g will be shown. Throughout this section we will face no necessity for assuming any particular form of $g(\sigma)$ like Eq. (2.8) and Eq. (2.9), rather we will keep g as a general function of σ .

3.1 Derivation

The δN formulation enables us to calculate super-horizon curvature perturbation (ζ) in terms of super-horizon field perturbations. It tells us that δN , i.e the difference in the number of e -foldings in different disconnected Hubble patches, is equal to the curvature perturbation on uniform density hyper-surface. So, for the model of our consideration we can write down,

$$\zeta = \delta N = N_\phi\delta\phi + N_\chi\delta\chi + N_\sigma\delta\sigma + \frac{1}{2}N_{\chi\chi}\delta\chi^2 + \frac{1}{2}N_{\sigma\sigma}\delta\sigma^2 , \quad (3.1)$$

¹ During inflation χ field does not get any super-horizon perturbation. It is because for efficient preheating g has to be around $10^5 m^2$ and this value of g makes χ heavy at the time of inflation [18]

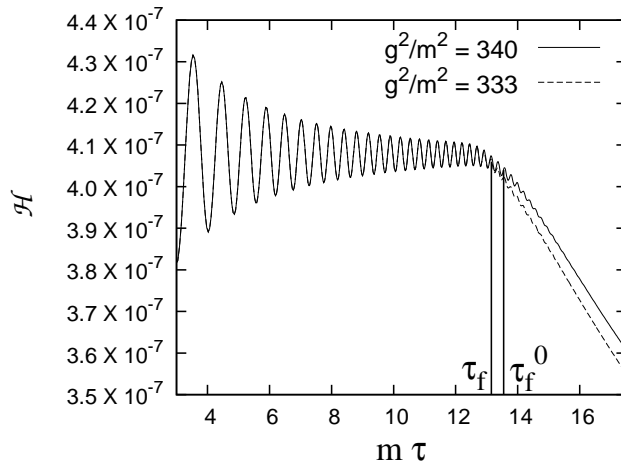


Figure 2. Trajectories of \mathcal{H} for different g values plotted using lattice simulation.

where any subscript denotes derivative with respect to that field. Here we have assumed that during preheating inflaton does not produce any second order perturbation[18, 23, 24]. For the $m^2\phi^2$ model in our present paper, we do not have to consider the contribution arising from the perturbations of χ , since χ does not get super-horizon perturbation during inflation. Therefore our main objective would be to calculate N_σ and $N_{\sigma\sigma}$.

In δN formulation [25–27] the difference in the value of the N should be taken on a uniform density hyper surface. So, for different initial conditions we have to see the evolution of different Hubble patches up to a certain Hubble value, not up to a fixed physical time. Here we use the formulation developed in [24] to calculate δN in this uniform density gauge. We take two different values of the coupling constant between ϕ and χ , one is g_0 and another is g . Then we see the evolution of Hubble trajectories with time in two different Hubble patches for these two different coupling constants. We write down

$$\delta N = \int_0^{t_e} H dt - \int_0^{t_e^0} H_0 dt , \quad (3.2)$$

where H is the Hubble parameter for g and H_0 is for g_0 and both the Hubble trajectories reach a uniform value H_e in time t_e and t_e^0 . Zero in subscript or superscript denotes the trajectory for coupling constant g_0 . Neglecting the gradient energy term, the Friedmann equation can be written as

$$\dot{H} + 3H^2 = 8\pi V(t). \quad (3.3)$$

If we change the variables to

$$\begin{aligned} \mathcal{H} &= a^{\frac{3}{2}} H , \\ \mathcal{V} &= a^3 V , \\ d\tau &= dt/a^{\frac{3}{2}} \end{aligned} \quad (3.4)$$

Eq. (3.3) takes the form

$$\frac{d\mathcal{H}}{d\tau} + \frac{3}{2}\mathcal{H}^2 = 8\pi\mathcal{V}. \quad (3.5)$$

Now we break up the integration limits in the Eq. (3.2). Let us say preheating ends at a rescaled time τ_f , much earlier than the final integration limit τ_e . For the g_0 trajectory these times are τ_f^0 and τ_e^0 respectively. Therefore we can rewrite Eq. (3.2) as

$$\delta N = \int_0^{\tau_f^0} (\mathcal{H}(g, \tau) - \mathcal{H}(g_0, \tau)) d\tau + \int_{\tau_f}^{\tau_e} \mathcal{H}(g, \tau) d\tau + \int_{\tau_f^0}^{\tau_f} \mathcal{H}(g, \tau) d\tau - \int_{\tau_f^0}^{\tau_e^0} \mathcal{H}(g_0, \tau) d\tau, \quad (3.6)$$

During the period from τ_f to τ_e , we need to take a particular dependence of the scale factor a with the physical time t . If w is the equation of state parameter, the continuity equation,

$$\dot{\rho} + 3H(1+w)\rho = 0, \quad (3.7)$$

and the definition of Hubble parameter, $H^2 = \frac{8\pi}{3}\rho$, provide us the dependence of H on physical time t . After writing Eq. (3.7) in the form of a differential equation of H and integrating it from t_f to t we get

$$\frac{1}{H} = \frac{1}{H_f} + \frac{1}{\alpha}(t - t_f), \quad (3.8)$$

where $\alpha = \frac{2}{3(1+w)}$. Further integrating over time within the same limits we find

$$a(t) = \left(a_f^{1/\alpha} + ct - ct_f \right)^\alpha, \quad (3.9)$$

where $c = \frac{H_f a_f^{1/\alpha}}{\alpha}$ is a constant. This form of $a(t)$ leads us to write

$$\int_{\tau_f}^{\tau_e} \mathcal{H} d\tau = -\alpha \log H_e + \alpha \log \mathcal{H}_f - \frac{3}{2}\alpha \log a_f. \quad (3.10)$$

We know $\log a_f = \int_0^{\tau_f} \mathcal{H} d\tau$. Again if $\tau_f < \tau_f^0$ we can write

$$\int_0^{\tau_f^0} \mathcal{H} d\tau = \int_0^{\tau_f} \mathcal{H} d\tau + \int_{\tau_f}^{\tau_f^0} \mathcal{H} d\tau \quad (3.11)$$

By using Eq. (3.10) and Eq. (3.11) we can recast Eq. (3.6) into

$$\delta N = \underbrace{\left(1 - \frac{3}{2}\alpha\right) \int_0^{\tau_f} (\mathcal{H} - \mathcal{H}_0) d\tau}_{\delta N_1} + \underbrace{\left(1 - \frac{3}{2}\alpha\right) \int_{\tau_f^0}^{\tau_f} \mathcal{H} d\tau}_{\delta N_2} + \underbrace{\alpha \log \frac{\mathcal{H}_f}{\mathcal{H}_f^0}}_{\delta N_3}, \quad (3.12)$$

Now let us evaluate the terms of Eq. (3.12) one by one. First we write

$$\delta N_1 = \left(1 - \frac{3}{2}\alpha\right) \int_0^{\tau_f} (\mathcal{H} - \mathcal{H}_0) d\tau = \left(1 - \frac{3}{2}\alpha\right) \int_0^{\tau_f} \Delta \mathcal{H}_i e^{\Lambda \tau} d\tau \quad (3.13)$$

where Λ is the Lyapunov exponent which describes the amount of separation between the trajectories with time. In the same equation $\Delta \mathcal{H}_i$ is the initial difference between the Hubble trajectories. In Fig. 2 we see that the trajectories with different g values bend downward at different τ . It means that for one of the g values, preheating takes larger time than the others. In Ref [24] it was shown that for different initial χ values, the final value of \mathcal{V} changes. This shift in the final value of \mathcal{V} is called node shift. Here for different initial g values the node shift is negligibly small. That is why we do not have to use any correction term

with the $\Delta\mathcal{H}_i$. It is because as g increases, the saturation value of X decreases [21] and ultimately the final value of $g^2\Phi^2X^2$ remains almost invariant of g . So the value of \mathcal{V} at the end of preheating (\mathcal{V}_f) does not change substantially for the variation in g . We can understand that since the initial value of X^2 is negligibly small compared to Φ^2 , a change in g would lead to very small value of $\Delta\mathcal{H}_i$. Still a large positive Lyapunov exponent can bifurcate the Hubble trajectories and Eq. (3.13) can get a large value.

Therefore we check the value of Lyapunov exponent, Λ . From the definition of Lyapunov exponent[28], we find

$$\Lambda(\tau) = \frac{1}{\tau} \int_0^\tau \log \left(1 - 3\mathcal{H} + 8\pi \frac{\partial\mathcal{V}}{\partial\mathcal{H}} \right) d\tau'. \quad (3.14)$$

from Eq. (3.5). So,

$$\int \Delta\mathcal{H}_i e^{\Lambda\tau} d\tau \approx \int \Delta\mathcal{H}_i \left[\exp \int \left(-3\mathcal{H} + 8\pi \frac{\partial\mathcal{V}}{\partial\mathcal{H}} - \frac{3}{2}\mathcal{H} \right) d\tau \right] dt \quad (3.15)$$

But $\mathcal{H}^2 = \frac{8\pi}{3}(\mathcal{V} + \mathcal{K})$, where $\mathcal{K} = a^3K$ the rescaled kinetic energy, and \mathcal{V} and \mathcal{K} are of same order in preheating era. So, $2\mathcal{H} = \frac{8\pi}{3} \left(\frac{\partial\mathcal{V}}{\partial\mathcal{H}} + \frac{\partial\mathcal{K}}{\partial\mathcal{H}} \right)$. So $3\mathcal{H}$ can be approximated as $8\pi \frac{\partial\mathcal{V}}{\partial\mathcal{H}}$. Therefore

$$\int \Delta\mathcal{H}_i e^{\Lambda\tau} d\tau \approx \int \Delta\mathcal{H}_i e^{\int -\frac{3}{2}\mathcal{H}d\tau} dt. \quad (3.16)$$

Eq. (3.16) indicates that the distance between the Hubble trajectories would exponentially decrease with time and since there is no such node shift, ultimately the total integration in Eq. (3.16) will produce negligible amount of δN .

Since g changes due to the change in σ , the third term in the RHS of Eq. (3.12) can be written as

$$\delta N_3 = \alpha \log \frac{\mathcal{H}_f}{\mathcal{H}_f^0} = \alpha \frac{\partial \log \mathcal{H}^f}{\partial \log g} \frac{g'}{g} \delta\sigma. \quad (3.17)$$

We have already mentioned that \mathcal{V}_f is independent of g . Since \mathcal{K}_f and \mathcal{V}_f are of the same order, \mathcal{H}_f does not change with g . Therefore δN_3 would be negligible. So, the dominant contribution to δN will arise from δN_2 defined in Eq. (3.12). Therefore we can write δN_2 as δN_{MP} , where the subscript ‘‘MP’’ denotes modulated preheating. Using Eq. (3.10), we can write it as

$$\begin{aligned} \delta N_2 = \delta N_{\text{MP}} &= \left(1 - \frac{3}{2}\alpha \right) \int_{\tau_f^0}^{\tau_f} \mathcal{H} d\tau \\ &= \alpha_1 \left(1 - \frac{3}{2}\alpha \right) \frac{\partial \log H^f}{\partial \log g} \frac{g'}{g} \delta\sigma \\ &= \alpha_1 \left(1 - \frac{3}{2}\alpha \right) \left[\underbrace{\frac{\partial \log \mathcal{H}^f}{\partial \log g}}_0 + \frac{3}{2} \frac{\partial \log a_f}{\partial \log g} \right] \frac{g'}{g} \delta\sigma \\ &= \left(1 - \frac{3}{2}\alpha \right) \frac{\partial \log a_f}{\partial \log g} \frac{g'}{g} \delta\sigma. \end{aligned} \quad (3.18)$$

Here during the period τ_f to τ_f^0 the form of $a(t)$ has been taken to be in the form of Eq. (3.9) with α replaced by α_1 . In the last line of Eq. (3.18), it is assumed that during preheating α_1 is almost equal to $\frac{2}{3}$.

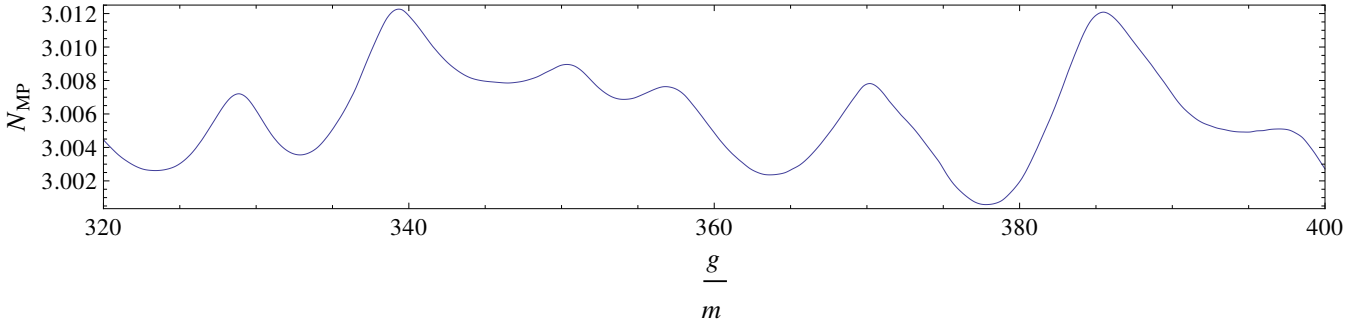


Figure 3. N_{MP} denotes the number of e -foldings during preheating period and after the end of preheating until Hubble parameter H reaches the final value H_e . This plot has been produced using lattice simulation, details of which has been described in appendix A

Although we have obtained an expression for δN_{MP} in Eq. (3.18), it is impossible to calculate the value for a particular choice of g analytically. It is because a_f is a function of the Floquet exponent μ_k [19] and μ_k is not known as a function of g . So, we have used lattice simulation to obtain the exact values of δN_{MP} for different values of g . We have performed the simulation of preheating process for $\frac{g}{m}$ from 320 to 400 with 1000 intermediate points. The simulations are run until the Hubble parameter reaches a particular value, say H_e . Since δN_{MP} does not depend on the particular choice of H_e , any value of it is fine as long as it is taken much after the end of preheating. The change of N_{MP} with $\frac{g}{m}$ is shown in Fig. 3. Numerical details of the lattice simulation is given in Appendix A.

We would like to check whether this expression of δN_{MP} gives a correct result. So we perform an order of magnitude estimation of the quantities of both sides in Eq. (3.18) with lattice simulation. First we take $a_f = (1 + \frac{3}{2}H_i t_f)^{\frac{2}{3}}$ and then from Eq. (3.18) we can write

$$\frac{3}{2}\delta N_{\text{MP}} = \left(1 - \frac{3}{2}\alpha\right) \delta \log\left(1 + \frac{3}{2}H_i t_f\right). \quad (3.19)$$

From lattice simulation we have also calculated the difference between mt_f for two $\frac{g}{m}$ values. For this purpose we choose two nearby g values for which δN_{MP} is maximum. There is a local maxima at $\frac{g}{m} = 340$ and a local minima at $\frac{g}{m} = 333$. We found that for $\frac{g}{m}$ values 333 and 340, the values of mt_f are 83 and 90 respectively. If we take α to be $\frac{1}{2}$ then $(1 - \frac{3}{2}\alpha) \delta \log(1 + \frac{3}{2}H_i t_f)$ becomes 0.018. This is the semi-analytical result calculated using Eq. (3.18) and putting the value of t_f from lattice simulation.

δN_{MP} could be calculated directly from Fig. 3. For the values of $\frac{g}{m}$ mentioned in the previous paragraph, we get from lattice result of Fig. 3

$$\frac{3}{2}\delta N_{\text{MP}} = \frac{3}{2}(N_{\text{MP}}(340) - N_{\text{MP}}(333)) = 0.012. \quad (3.20)$$

Since this is the same order of magnitude as the semi-analytical result derived earlier, we conclude that Eq. (3.18) gives correct estimation.

Now we would like to compare our work with a similar work done earlier in Ref. [19]. For that we need to write Eq. (3.18) in terms of curvature perturbation generated by modulated reheating. In modulated reheating, curvature perturbation takes the following form [3, 4],

$$\zeta = \delta N_{\text{MR}} = -\frac{1}{6} \frac{\delta \Gamma}{\Gamma} = -\frac{2}{3} \frac{\delta g}{g}, \quad (3.21)$$

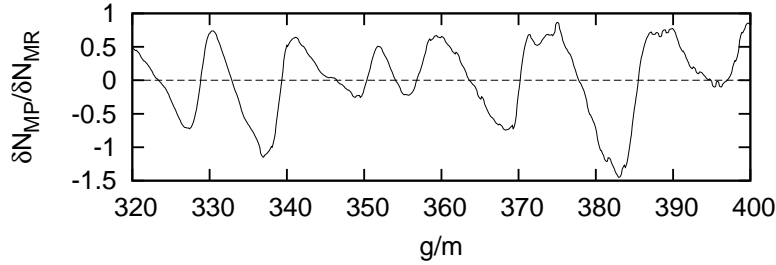


Figure 4. As g/m changes the ratio of the curvature perturbations generated in two different processes gets both negative and positive values.

where Γ is the decay rate from ϕ to χ . Subscript “MR” denotes modulated reheating. Using this we can write

$$\delta N_{\text{MP}} = g \frac{\partial N_{\text{MP}}}{\partial g} \frac{\delta g}{g} = -\frac{3}{2} g \frac{\partial N_{\text{MP}}}{\partial g} \delta N_{\text{MR}}. \quad (3.22)$$

$\frac{\partial N_{\text{MP}}}{\partial g}$ has been calculated from Fig. 3 and the ratio of δN_{MP} to δN_{MR} has been plotted in Fig. 4. We can also write Eq. (3.22) using Eq. (3.19) and $\alpha = \frac{1}{2}$ as

$$\delta N_{\text{MP}} = -\frac{1}{4} \frac{\partial \log(1 + \frac{3}{2} H_i t_f)}{\partial \log g} \delta N_{\text{MR}}. \quad (3.23)$$

There are some differences between our result and that obtained in [19]. There are two reasons behind this. In the case of analytical calculations the authors of Ref. [19] did not calculate δN in uniform density gauge. That means difference between two values N_{MP} for two different values of $\frac{g}{m}$ was not taken at fixed final Hubble value H_e . Rather they have fixed a final time. The final time t in Eq. (3.1) of Ref. [19] is treated as independent of g . But in uniform density gauge final Hubble value should remain constant whereas the final time should vary. Therefore in their estimation they got almost double the value than the expression shown in Eq. (3.23). The second reason is coming from the fact that efficiency of lattice simulation in considering backreaction is much better than any other semi-analytical estimation. That is why estimations of final time (t_f) in these two methods are bound to be different, and consequently the earlier study [19] has shown a large ratio of δN_{MP} to δN_{MR} than the lattice result shown in Fig. 4.

We learn from these two plots, Fig. 3 and Fig. 4, that the curvature perturbation generated by modulated preheating is not large compared to that generated by modulated reheating. As far as the amplitude of curvature perturbation is concerned, modulated preheating is indistinguishable from modulated reheating.

3.2 Constraints

We have seen in Fig. 3 that N_{MP} does not have any simple dependence on g from where we could directly constrain its variation. Therefore to constrain the variation in g , we have taken a set of 10000 randomly different values of $\frac{g^2}{m^2}$ and variation in $\frac{g^2}{m^2}$ (say $\Delta \frac{g^2}{m^2}$) in Fig. 5. The set has been generated with log-uniform distribution in two dimensional parameter space of $\frac{g^2}{m^2}$ and $\Delta \frac{g^2}{m^2}$. For $\frac{g^2}{m^2}$ the range was 10^5 to 10^6 and for $\Delta \frac{g^2}{m^2}$ the range was 1 to 100. From lattice simulation of Fig. 3 we have generated the absolute values of δN_{MP} as

$$\delta N_{\text{MP}} = \left| N_{\text{MP}} \left(\frac{g^2}{m^2} + \Delta \frac{g^2}{m^2} \right) - N_{\text{MP}} \left(\frac{g^2}{m^2} \right) \right| \quad (3.24)$$

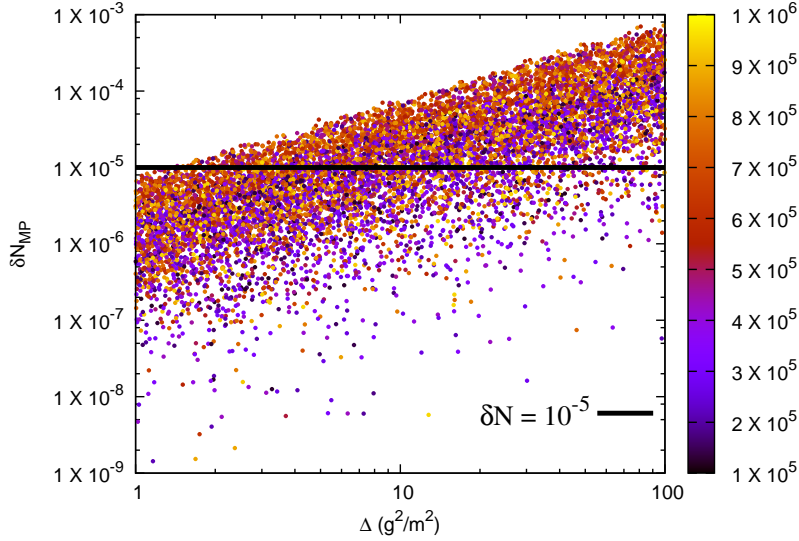


Figure 5. To keep the value of δN under the observed bound of 10^{-5} , variation in $\frac{g^2}{m^2}$ should be about $\mathcal{O}(1)$. Different colour represents different values of $\frac{g^2}{m^2}$ around which the variation has been taken.

From Fig. 5 we see that in order to keep δN_{MP} within observational bound [29] which is $\mathcal{O}(10^{-5})$, variation in $\frac{g^2}{m^2}$ has to be within $\mathcal{O}(1)$. Otherwise to keep δN_{MP} within observational limit we have to fine tune g . That means if $\Delta\frac{g^2}{m^2}$ is of around $\mathcal{O}(10)$ we may still have δN_{MP} under 10^{-5} but we have to choose $\frac{g^2}{m^2}$ arbitrarily with an accuracy of one part in 10^6 .

Let us compare this result to the constraint from modulated reheating. From Eq. (3.21) we can say that $\frac{\delta g}{g}$ has to be less than $\mathcal{O}(10^{-5})$. But in the case of modulated preheating, we have $\Delta\frac{g^2}{m^2} \leq \mathcal{O}(1)$ which means

$$\frac{\delta g}{g} \leq \frac{1}{2} \frac{m^2}{g^2}. \quad (3.25)$$

When we are taking $\frac{g^2}{m^2}$ around 10^5 both the mechanisms are basically giving the same constraint. For higher values of $\frac{g^2}{m^2}$ this constraint becomes tighter. This is one of the main features of modulated preheating. We have checked that in whatever range we take the values of $\frac{g^2}{m^2}$ (for example from 10^6 to 10^7), the constraint, $\Delta\frac{g^2}{m^2} \leq \mathcal{O}(1)$ remains unchanged.

4 Iso-curvature perturbation

In this section we derive a constraint on the value of $\langle\sigma\rangle^*$. We can think of σ as a cold dark matter candidate if its mass is very small. In this case, when the Hubble parameter drops down to a value which is much less than the mass of σ , $\langle\sigma\rangle$ would oscillate around the minima of its potential. This kind of oscillating scalar field behaves like a bosonic condensate and can be considered as dark matter [30]. This scenario would generate iso-curvature perturbations whose amplitude in uniform density gauge (the same gauge in which the δN formulation is defined) would be [19],

$$\mathcal{S} \approx 2 \frac{\delta\sigma}{\langle\sigma\rangle^*}, \quad (4.1)$$

where the value of $\delta\sigma$ and $\langle\sigma\rangle^*$ should be taken at the time of the horizon exit of the largest mode in CMB. This form of iso-curvature perturbation in Eq. (4.1) comes from the fact that we have assumed σ to have a potential term like $\frac{1}{2}m_\sigma^2\sigma^2$. Since we are also assuming in this paper that most of the curvature perturbations are generated by inflaton fluctuations during inflation, the iso-curvature perturbations will be un-correlated to the curvature perturbations. Therefore we can say that $\delta\sigma$ is of the order of H^* , which is the value of Hubble at the time of horizon exit of the largest mode in CMB. Iso-curvature ratio is defined as [31–33]

$$\alpha_{\text{iso}} = \frac{\mathcal{P}_S}{\mathcal{P}_S + \mathcal{P}_\zeta} = \frac{\frac{4}{\langle\sigma\rangle^{*2}} \left(\frac{H^*}{2\pi}\right)^2}{\frac{4}{\langle\sigma\rangle^{*2}} \left(\frac{H^*}{2\pi}\right)^2 + \mathcal{P}_\zeta}, \quad (4.2)$$

where \mathcal{P}_S and \mathcal{P}_ζ are the amplitudes of the power spectrums of iso-curvature and curvature perturbations respectively. H^* has a value of 6×10^{-6} for our model where m has been taken to be 10^{-6} . \mathcal{P}_ζ is fixed at 2.2×10^{-9} from observations [34]. Observational bound limits the value of α_{iso} to be less than 0.038 [34]. So, $\langle\sigma\rangle$ has to be taken such that α_{iso} remains well within the observational limit. Therefore in order to satisfy this limit we have to take,

$$\langle\sigma\rangle^* \geq 0.2. \quad (4.3)$$

There is a concern about this mechanism of generating the iso-curvature perturbations. It has been shown in Ref. [35] that if the universe undergoes an era of local thermal equilibrium, the super-horizon non-adiabatic perturbations generated prior to that era would become adiabatic. After the end of preheating, the classical background value of ϕ decreases and its energy is used in producing χ and ϕ particles. These particles get thermalised within some time. But there is no mechanism which can allow the decay of $\langle\sigma\rangle$ to the constituent particles of the universe. That is why $\langle\sigma\rangle$ will remain decoupled from the thermal bath of the universe. At a later time when the value of Hubble parameter drops down significantly to make $\langle\sigma\rangle$ an oscillating scalar field around the minima of its potential, $\langle\sigma\rangle$ will start behaving like a condensate of zero momentum modes and it can become a dark matter candidate as in the case of axion dark matter [30]. In this scenario there is no era of complete local thermal equilibrium. So the iso-curvature modes are expected to show up in CMB.

But if this coherent oscillation of $\langle\sigma\rangle$ leads to the evaporation of the σ condensate, then the local thermal equilibrium will be restored again. But that depends on many different parameters, one of them being the number density of σ particles at that time. Therefore it is impossible to predict the fate of $\langle\sigma\rangle$ condensate without taking into account the complete thermal history of the universe.

In the following section we will discuss these two possibilities. First we will put this minimum value of $\langle\sigma\rangle^*$ in some particular functional form of $g(\sigma)$ and constrain other parameters of the theory from the observational limits of non-gaussianity. Then we will study the other case in which the constraint of Eq. (4.3) is relaxed.

5 Non-gaussianity

In this section we will derive the general expression of non-gaussianity parameter $f_{\text{NL}}^{\text{local}}$ in modulated preheating scenario. Then we will consider one by one the models of Eq. (2.9) and Eq. (2.8). After that we will try to put some constraints on the model parameters from observational results.

After picking out only the relevant terms from Eq. (3.1), the total curvature perturbation can be written in Fourier space as

$$\zeta_k = N_\phi \delta\phi_k + N_\sigma^{\text{MP}} \delta\sigma_k + \frac{1}{2} N_{\sigma\sigma}^{\text{MP}} \int \frac{d^3p}{(2\pi)^3} \delta\sigma_p \delta\sigma_{k-p}. \quad (5.1)$$

If the curvature perturbation generated from perturbation of ϕ and σ are uncorrelated, i.e., $\langle \zeta_k^\phi \zeta_k^\sigma \rangle = 0$, we can write the two-point correlation function and power-spectrum as

$$\langle \zeta_{k_1} \zeta_{k_2} \rangle = \langle \zeta_{k_1}^\phi \zeta_{k_2}^\phi \rangle + \langle \zeta_{k_1}^\sigma \zeta_{k_2}^\sigma \rangle, \quad (5.2)$$

$$\mathcal{P}_\zeta(k) = (N_\phi^2 + (N_\sigma^{\text{MP}})^2) \left(\frac{H^*}{2\pi} \right)^2. \quad (5.3)$$

Here we have neglected the higher order terms in $\delta\sigma$. We write the power spectrum of the curvature perturbations produced by modulated preheating as

$$\mathcal{P}_\zeta^{\text{MP}} = (N_\sigma^{\text{MP}})^2 \left(\frac{H^*}{2\pi} \right)^2. \quad (5.4)$$

Defining f_{NL} as the ratio of bi-spectrum to the squared of power spectrum [36–38] we get,

$$\begin{aligned} f_{\text{NL}}^{\text{local}} &= \frac{5}{3} \frac{\langle \zeta_{k_1} \zeta_{k_2} \zeta_{k_3} \rangle}{\langle \zeta_{k_1} \zeta_{k_2} \rangle^2 + \text{permutations}} \Big|_{k_1=k_2=k \gg k_3} \\ &= \frac{5}{6} (N_\sigma^{\text{MP}})^2 N_{\sigma\sigma}^{\text{MP}} \frac{\mathcal{P}_\sigma^2}{\mathcal{P}_\zeta^2}. \end{aligned} \quad (5.5)$$

Unlike modulated reheating, in the case of modulated preheating we cannot write down N_σ and $N_{\sigma\sigma}$ directly as a function of σ . Rather we can only write,

$$N_\sigma = N_g \frac{\partial g}{\partial \sigma}, \quad (5.6)$$

$$N_{\sigma\sigma} = N_g \frac{\partial^2 g}{\partial \sigma^2} + N_{gg} \left(\frac{\partial g}{\partial \sigma} \right)^2. \quad (5.7)$$

Here N_g and N_{gg} denotes first derivative and second derivative of N_{MP} (see Fig. 3) with respect to g . Therefore for the model of Eq. (2.9) we can recast Eq. (5.5) into

$$f_{\text{NL}}^{\text{local}} = \frac{5H^{*4} N_g^2 g^3 \langle \sigma \rangle^{*2}}{96M_2^4 \pi^4 \mathcal{P}_\zeta^2 (M_2^2 + \langle \sigma \rangle^{*2})^3} \left(M_2^2 N_{gg} g \langle \sigma \rangle^{*2} + N_{gg} g \langle \sigma \rangle^{*4} + M_2^4 N_g \sqrt{1 + \frac{\langle \sigma \rangle^{*2}}{M_2^2}} \right). \quad (5.8)$$

We have already said that in this paper that we assume curvature perturbations are mostly generated due to quantum fluctuations of the inflaton field during inflation. Therefore we put the value of \mathcal{P}_ζ to be 2.2×10^{-9} from observation [34]. Since N_{MP} behaves non-trivially with g in Fig. 3, N_g and N_{gg} also don't have any simple dependence on g . So we take the values of N_g and N_{gg} from lattice results of N_{MP} shown in Fig. 3. By plugging in the values of N_g, N_{gg}, M_2 and $\langle \sigma \rangle^*$ in Eq. (5.8) we can calculate the values of f_{NL} .

In table 1 we have demonstrated that for the same values of M_2 and $\langle \sigma \rangle^*$, f_{NL} can change drastically if we make a change of order one in the value of $\frac{g}{m}$. A small change in $\frac{g}{m}$ changes the parameters A_k

M_2	$\langle\sigma\rangle^*$	g/m	mN_g	m^2N_{gg}	f_{NL}
1×10^{-2}	0.2	322	-0.00048	0.00032	11.29
1×10^{-2}	0.2	323	0.00009	0.00030	0.38
1×10^{-2}	0.2	324	0.00017	0.00031	1.41

Table 1. For slightly different value of g , f_{NL} changes drastically, though M_2 and $\langle\sigma\rangle^*$ are kept fixed.

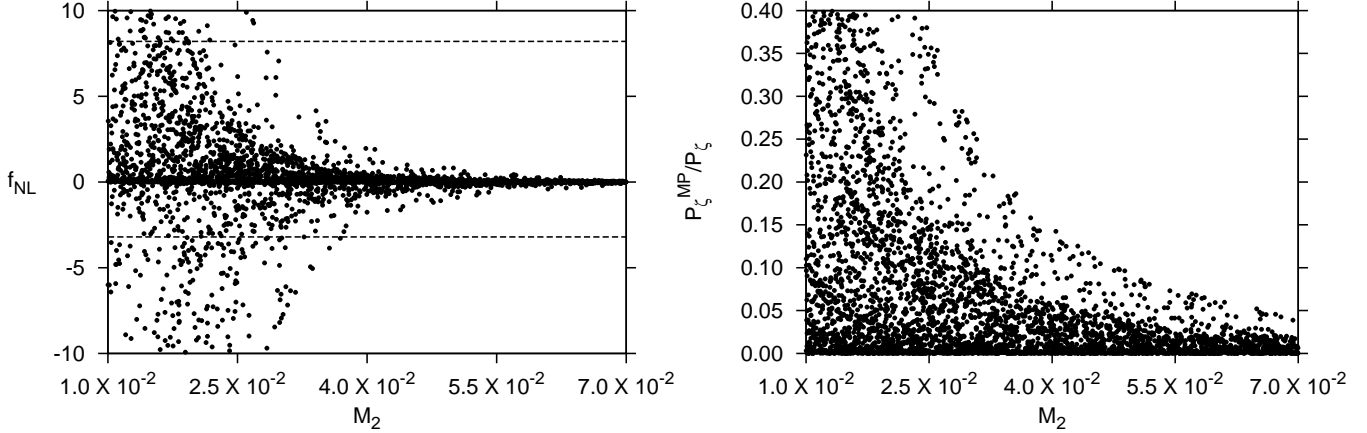


Figure 6. These plots are for $g^2 = g_0^2 \left(1 + \frac{\sigma^2}{M_2^2}\right)$. Different points in the plots represent different values of g and M_2 . The upper and lower dashed lines indicate the observational upper and lower limit of $f_{\text{NL}} = 2.5 \pm 5.7$. We see that to keep f_{NL} within the observational bound for arbitrary choice of g we need $M_2 \geq 4 \times 10^{-2}$. $\langle\sigma\rangle^*$ has been chosen to be 0.2 to keep amplitude of iso-curvature perturbation under observational constraint. We see that for that for values of M_2 above the threshold mentioned, $\mathcal{P}_\zeta^{\text{MP}}$ to \mathcal{P}_ζ remains under 0.13. Results are in $M_P = 1$ unit.

and q of Eq. (2.4). That is why the characteristic exponent (μ_k) also changes with the change in $\frac{g}{m}$. So, the modes which have undergone parametric resonance earlier might not experience resonance when $\frac{g}{m}$ is changed. This leads to a sudden change in the value of t_f . If the values of t_f obtained for two nearby values of $\frac{g}{m}$ are very different, N_g becomes large and the values of f_{NL} in Eq. (5.8) become widely different. Therefore the small change in $\frac{g}{m}$ can drag away the value of f_{NL} from its observational limit. Conversely, if the values of t_f for different $\frac{g}{m}$ are not very different, N_g and f_{NL} both remain small. Any theory would be unnatural if its parameter has to be fine tuned to $\mathcal{O}(1)$ in 300 to predict observed physical quantity. Therefore to bring out the simple conclusion from this complex dynamics we have taken help of scatter plots in the following way.

As done in subsection 3.2, we take a set of 10000 random values of $\frac{g}{m}$ and M_2 for the model in Eq. (2.9). The random values are generated with uniform distribution in the two dimensional parameter space of $\frac{g}{m}$ and M_2 where the range for $\frac{g}{m}$ is from 320 to 400 and the range for M_2 is from 1×10^{-2} to 8×10^{-2} . Then we fix $\langle\sigma\rangle^*$ to be 0.2. N_g and N_{gg} take different values for different $\frac{g}{m}$ as described in table 1. So f_{NL} becomes function of only $\frac{g}{m}$ and M_2 . In Fig. 6 we see that for different values of $\frac{g}{m}$, f_{NL} may behave arbitrarily, but there is a clear dependency of f_{NL} with M_2 as evident from Eq. (5.8). This ensures that if we want to avoid fine tuning of $\frac{g}{m}$ and still want to keep f_{NL} within observational limit 2.5 ± 5.7 [39], we need $M_2 \geq 4 \times 10^{-2}$. This result immediately translates into the fact that (see the right panel of Fig. 6) the amplitude of the power spectrum of curvature perturbation produced via modulated preheating will always remain within 13% of that of the total curvature perturbations.

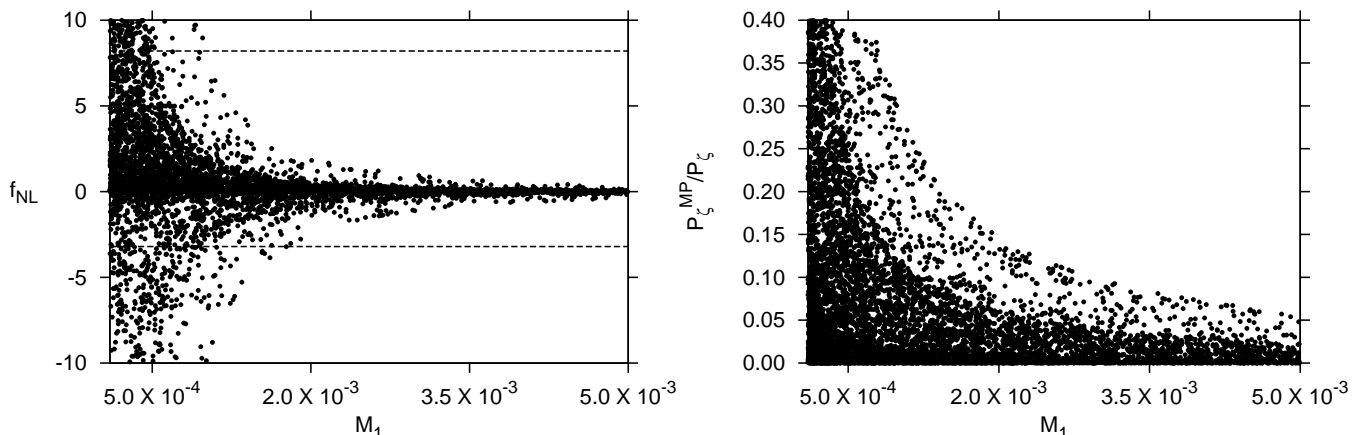


Figure 7. These plots are for $g^2 = g_0^2 \left(1 + \frac{\sigma}{M_1}\right)$. Different points in the plots represent different values of g and M_1 . The upper and lower dashed lines indicate the observational upper and lower limit of $f_{\text{NL}} = 2.5 \pm 5.7$. We see that to keep f_{NL} within the observational bound for arbitrary choice of g we need $M_1 \geq 2 \times 10^{-3}$. $\langle \sigma \rangle^*$ has been chosen to be 0.2 to keep amplitude of iso-curvature perturbation under observational constraint. We see that for that for values of M_1 above the threshold mentioned, $\mathcal{P}_\zeta^{\text{MP}}$ to \mathcal{P}_ζ remains under 0.15. Results are in $M_P = 1$ unit.

We repeat the same exercise for the model of Eq. (2.8). Here f_{NL} takes the following form

$$f_{\text{NL}}^{\text{local}} = \frac{5H^{*4}N_g^2g^2}{384M_1\pi^4P_\zeta^2(M_1 + \langle \sigma \rangle^*)} \left(-\frac{N_g g}{4M_1^2 \left(1 + \frac{\langle \sigma \rangle^*}{M_1}\right)^{3/2}} + \frac{N_{gg}g^2}{4M_1^2 \left(1 + \frac{\langle \sigma \rangle^*}{M_1}\right)} \right) \quad (5.9)$$

We find that we need $M_1 \geq 2 \times 10^{-3}$ and in this case amplitude of the power spectrum of curvature perturbations produced via modulated preheating remains below 15% of that of the total curvature perturbations(see Fig. 7).

We have discussed in the previous section, the iso-curvature perturbation may not show up in CMB if the universe has undergone an era of local thermal equilibrium. In that case, the constraint on the value of $\langle \sigma \rangle^*$ is not valid. Still we can draw some conclusions regarding the amount of curvature perturbations that can be allowed to be generated by modulated preheating. We see in Fig. 6 and Fig. 7 that the minimum acceptable values of M_1 and M_2 are much smaller than the fixed value of $\langle \sigma \rangle^*$. We have also understood from these figures that when M_1 and M_2 tend towards $\langle \sigma \rangle^*$, the ratio $\mathcal{P}_\zeta^{\text{MP}}/\mathcal{P}_\zeta$ becomes smaller. Because of this monotonic nature, it can be safely said that the upper bound on $\mathcal{P}_\zeta^{\text{MP}}/\mathcal{P}_\zeta$ need not be revised even if we take much higher values of M_1 and M_2 than what have been shown in the figures.

Now let us investigate the case where M_1 and M_2 are much smaller than $\langle \sigma \rangle^*$. We notice from Fig. 6 and Fig. 7 that the value of f_{NL} increases in this case. In this limit Eq. (5.5) can be written as

$$f_{\text{NL}}^{\text{local}} \approx \frac{5N_{gg}}{6N_g^2} \left(\frac{\mathcal{P}_\zeta^{\text{MP}}}{\mathcal{P}_\zeta} \right)^2. \quad (5.10)$$

In Fig. 8 we check how f_{NL} behaves with $\mathcal{P}_\zeta^{\text{MP}}/\mathcal{P}_\zeta$ for different values of g . Looking at the figure we see that the points in the plot predominantly appear in a band like region. For $\mathcal{P}_\zeta^{\text{MP}}/\mathcal{P}_\zeta < 0.01$ this band lies within the allowed range of $|f_{\text{NL}}|$. Thus the constraint in this case becomes tighter compared to earlier cases where the corresponding maximum value of $\mathcal{P}_\zeta^{\text{MP}}/\mathcal{P}_\zeta$ was 0.13 and 0.15 respectively. Combining all cases we now conclude that the maximum allowed value of $\mathcal{P}_\zeta^{\text{MP}}/\mathcal{P}_\zeta$ is 0.15.

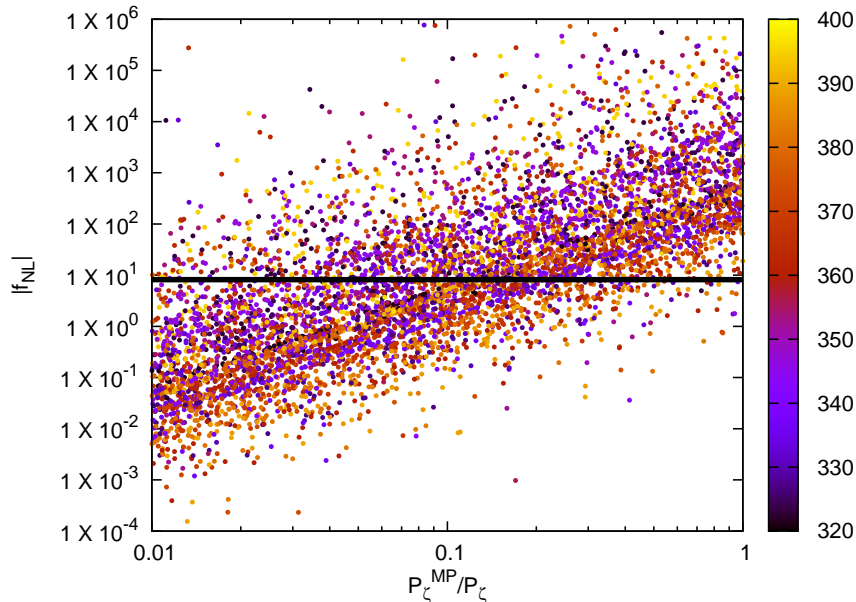


Figure 8. For M_1 and M_2 much smaller than $\langle\sigma\rangle^*$ the amount of curvature perturbation generated by modulated preheating has to be less than 1% of the total curvature perturbations to keep the absolute value of $f_{\text{NL}}^{\text{local}}$ within the observational upper limit. The line shows the observational upper limit of $f_{\text{NL}}^{\text{local}} = 8.2$. Different colours represent different $\frac{g}{m}$ values.

6 Conclusion

In this paper we have studied, both semi-analytically and numerically, the effects that can be produced in CMB if the coupling of the inflaton with another scalar field varies on super horizon scales. Modulated reheating mechanism has been thought of producing total observed CMB perturbations. But here we have shown that its non-perturbative extension, modulated preheating, is not fit for that purpose. If modulated preheating has to be responsible for producing substantial large amount of observed density perturbation in CMB and at the same time it has to keep the iso-curvature perturbations and local form non-gaussianity within observational limit, the parameters of the theory have to be unnaturally fine tuned. Only for certain lower bound on the mass scales related to the modulating field the theory becomes natural. But this lower bound on the mass scales immediately dictates that modulated preheating mechanism can at maximum be responsible for generating 15% of the observed CMB fluctuations.

If the iso-curvature perturbations become adiabatic during the evolution of the universe, the lower bound on the background value of the modulating field ($\langle\sigma\rangle^*$) does not hold. Consequently the lower bounds on mass scales M_1 and M_2 can not be derived. But that could not relax the upper limit on the allowed amount of curvature perturbations produced by modulated preheating mechanism. For any value of $\langle\sigma\rangle^*$ there are two possibilities. First is that the cutoff scales M_1 and M_2 are much smaller than $\langle\sigma\rangle^*$ and second possibility is the opposite of it. For the first category the modulated preheating can generate 1% of the observed CMB fluctuations at maximum if the absolute value of f_{NL} has to remain with observational limit, while for the second category it can go up to around 13% or 15% depending on the model.

From the point of view of model building the lower bound on mass scales M_1 and M_2 is expected to be very useful. As we have discussed that in different models this scales come from different physics. In string-related models these scales come from the compactification of some higher dimensions. In particle physics models these scales corresponds to the mass of intermediate particles in the theory. Therefore

constraints on M_1 and M_2 would indirectly provide bounds on the physics behind producing modulated coupling constant. These constraints on M_1 and M_2 would be always applicable as long as inflaton potential can be assumed to be like $m^2\phi^2$ near its minima and inflaton's energy decays into another scalar field.

Moreover we have developed a semi-analytical method for calculating the order of the amplitude of the curvature perturbation produced by this mechanism. We have been able to supply the lattice results of the dependence of number of e -foldings during preheating era on the coupling constant of inflaton and a secondary scalar field. Therefore if there is a different model which has different dependence of coupling constant with the vev of a scalar field other than those discussed in our work, one can, in principle, use the lattice result to put a constraint on the cutoff scales for that framework.

A Numerical details

Lattice simulation has been done using the publicly available code LATTICEEASY[40]. We have taken a 32^3 lattice which means a 3-dimensional lattice with 32 points along each edge. Length of the each side of lattice has been taken to be $20H_i$, where H_i is the Hubble parameter at the start of the simulation. For our case H_i has the value of 4.9×10^{-7} and the value of m has been fixed at 10^{-6} . Time step in mt was taken to be 0.001. Along with the double precession, this time step provides an energy conservation accuracy(ECA) of the order of 10^{-4} . Since the variation of δN with g is smooth and not spiky like the case with the variation of initial background value of χ [23], this ECA is sufficient to provide right accuracy for the simulation.

Simulation terminates for each choice of $\frac{g}{m}$ at a particular final Hubble parameter(H_e) which has been taken to be 4.402×10^{-9} . But it has been proved in Eq. (3.12) that δN is practically independent of the value of H_e as long as it denotes a Hubble parameter in radiation domination phase. Therefore different choices of H_e can lead to an overall change in N_{MP} but not in $\delta N_{\text{MP}}, N_g$ or N_{gg} . So, the values obtained for the observable quantities are also independent of H_e .

Acknowledgement

AM would like to thank Palash B Pal for various important discussions and suggestions. The authors acknowledge the Department of Atomic Energy (DAE, Govt. of India) for financial assistance.

References

- [1] A. D. Linde, *A New Inflationary Universe Scenario: A Possible Solution of the Horizon, Flatness, Homogeneity, Isotropy and Primordial Monopole Problems*, *Phys.Lett.* **B108** (1982) 389–393.
- [2] A. D. Linde, *Scalar Field Fluctuations in Expanding Universe and the New Inflationary Universe Scenario*, *Phys.Lett.* **B116** (1982) 335.
- [3] G. Dvali, A. Gruzinov and M. Zaldarriaga, *Cosmological perturbations from inhomogeneous reheating, freezeout, and mass domination*, *Phys.Rev.* **D69** (2004) 083505, [[astro-ph/0305548](#)].
- [4] G. Dvali, A. Gruzinov and M. Zaldarriaga, *A new mechanism for generating density perturbations from inflation*, *Phys.Rev.* **D69** (2004) 023505, [[astro-ph/0303591](#)].
- [5] F. Vernizzi, *Cosmological perturbations from varying masses and couplings*, *Phys. Rev.* **D69** (2004) 083526, [[astro-ph/0311167](#)].
- [6] N. Kobayashi, T. Kobayashi and A. L. Erickcek, *Rolling in the Modulated Reheating Scenario*, *JCAP* **1401** (2014) 036, [[1308.4154](#)].
- [7] F. Bernardeau, L. Kofman and J.-P. Uzan, *Modulated fluctuations from hybrid inflation*, *Phys. Rev.* **D70** (2004) 083004, [[astro-ph/0403315](#)].

- [8] M. Cicoli, G. Tasinato, I. Zavala, C. Burgess and F. Quevedo, *Modulated Reheating and Large Non-Gaussianity in String Cosmology*, *JCAP* **1205** (2012) 039, [[1202.4580](#)].
- [9] K. Enqvist, A. Mazumdar and M. Postma, *Challenges in generating density perturbations from a fluctuating inflaton coupling*, *Phys.Rev.* **D67** (2003) 121303, [[astro-ph/0304187](#)].
- [10] L. Kofman, *Probing string theory with modulated cosmological fluctuations*, [astro-ph/0303614](#).
- [11] N. S. Sugiyama, E. Komatsu and T. Futamase, *The δN Formalism*, *Phys.Rev.* **D87** (2013) 023530, [[1208.1073](#)].
- [12] D. H. Lyth, K. A. Malik and M. Sasaki, *A General proof of the conservation of the curvature perturbation*, *JCAP* **0505** (2005) 004, [[astro-ph/0411220](#)].
- [13] D. H. Lyth and Y. Rodriguez, *The Inflationary prediction for primordial non-Gaussianity*, *Phys.Rev.Lett.* **95** (2005) 121302, [[astro-ph/0504045](#)].
- [14] M. Zaldarriaga, *Non-Gaussianities in models with a varying inflaton decay rate*, *Phys.Rev.* **D69** (2004) 043508, [[astro-ph/0306006](#)].
- [15] K. Ichikawa, T. Suyama, T. Takahashi and M. Yamaguchi, *Primordial Curvature Fluctuation and Its Non-Gaussianity in Models with Modulated Reheating*, *Phys. Rev.* **D78** (2008) 063545, [[0807.3988](#)].
- [16] T. Suyama, T. Takahashi, M. Yamaguchi and S. Yokoyama, *Implications of Planck results for models with local type non-Gaussianity*, *JCAP* **1306** (2013) 012, [[1303.5374](#)].
- [17] K.-Y. Choi and O. Seto, *Modulated reheating by curvaton*, *Phys. Rev.* **D85** (2012) 123528, [[1204.1419](#)].
- [18] K. Kohri, D. H. Lyth and C. A. Valenzuela-Toledo, *Preheating and the non-gaussianity of the curvature perturbation*, *JCAP* **1002** (2010) 023, [[0904.0793](#)].
- [19] K. Enqvist and S. Rusak, *Modulated preheating and isocurvature perturbations*, *JCAP* **1303** (2013) 017, [[1210.2192](#)].
- [20] L. Ackerman, C. W. Bauer, M. L. Graesser and M. B. Wise, *Light scalars and the generation of density perturbations during preheating or inflaton decay*, *Phys.Lett.* **B611** (2005) 53–59, [[astro-ph/0412007](#)].
- [21] L. Kofman, A. D. Linde and A. A. Starobinsky, *Towards the theory of reheating after inflation*, *Phys.Rev.* **D56** (1997) 3258–3295, [[hep-ph/9704452](#)].
- [22] G. N. Felder and L. Kofman, *The Development of equilibrium after preheating*, *Phys. Rev.* **D63** (2001) 103503, [[hep-ph/0011160](#)].
- [23] J. R. Bond, A. V. Frolov, Z. Huang and L. Kofman, *Non-Gaussian Spikes from Chaotic Billiards in Inflation Preheating*, *Phys.Rev.Lett.* **103** (2009) 071301, [[0903.3407](#)].
- [24] A. Mazumdar and K. P. Modak, *Deriving super-horizon curvature perturbations from the dynamics of preheating*, *JCAP* **1504** (2015) 053, [[1412.8522](#)].
- [25] N. Bartolo, S. Matarrese and A. Riotto, *Enhancement of non-Gaussianity after inflation*, *JHEP* **0404** (2004) 006, [[astro-ph/0308088](#)].
- [26] A. Chambers and A. Rajantie, *Non-Gaussianity from massless preheating*, *JCAP* **0808** (2008) 002, [[0805.4795](#)].
- [27] A. Chambers and A. Rajantie, *Lattice calculation of non-Gaussianity from preheating*, *Phys.Rev.Lett.* **100** (2008) 041302, [[0710.4133](#)].
- [28] S. H. Strogatz, *Nonlinear dynamics and chaos*, Westview Press (1994) .
- [29] D. Larson, J. Dunkley, G. Hinshaw, E. Komatsu, M. Nolta et al., *Seven-Year Wilkinson Microwave Anisotropy Probe (WMAP) Observations: Power Spectra and WMAP-Derived Parameters*, *Astrophys.J.Suppl.* **192** (2011) 16, [[1001.4635](#)].
- [30] J. Preskill, M. B. Wise and F. Wilczek, *Cosmology of the Invisible Axion*, *Phys. Lett.* **B120** (1983) 127–132.

- [31] M. Beltran, *Isocurvature, non-gaussianity and the curvaton model*, *Phys.Rev.* **D78** (2008) 023530, [[0804.1097](#)].
- [32] A. R. Liddle and D. H. Lyth, *The Cold dark matter density perturbation*, *Phys.Rept.* **231** (1993) 1–105, [[astro-ph/9303019](#)].
- [33] C. Gordon, D. Wands, B. A. Bassett and R. Maartens, *Adiabatic and entropy perturbations from inflation*, *Phys.Rev.* **D63** (2001) 023506, [[astro-ph/0009131](#)].
- [34] PLANCK collaboration, P. A. R. Ade et al., *Planck 2015 results. XX. Constraints on inflation*, [1502.02114](#).
- [35] S. Weinberg, *Must cosmological perturbations remain non-adiabatic after multi-field inflation?*, *Phys. Rev.* **D70** (2004) 083522, [[astro-ph/0405397](#)].
- [36] E. Komatsu, *The pursuit of non-gaussian fluctuations in the cosmic microwave background*, [astro-ph/0206039](#).
- [37] N. Bartolo, E. Komatsu, S. Matarrese and A. Riotto, *Non-Gaussianity from inflation: Theory and observations*, *Phys.Rept.* **402** (2004) 103–266, [[astro-ph/0406398](#)].
- [38] M. Liguori, F. Hansen, E. Komatsu, S. Matarrese and A. Riotto, *Testing primordial non-gaussianity in cmb anisotropies*, *Phys.Rev.* **D73** (2006) 043505, [[astro-ph/0509098](#)].
- [39] PLANCK collaboration, P. A. R. Ade et al., *Planck 2015 results. XVII. Constraints on primordial non-Gaussianity*, [1502.01592](#).
- [40] G. N. Felder and I. Tkachev, *LATTICEEASY: A Program for lattice simulations of scalar fields in an expanding universe*, *Comput.Phys.Commun.* **178** (2008) 929–932, [[hep-ph/0011159](#)].

